ChemComm

COMMUNICATION

Unimolecular Thermometers: Core-Shell Polymer Bottlebrushes with Solvatochromic Responses to Temperature

Received 00th January 20xx,
Accepted 00th January 20xx

DOI: 10.1039/x0xx00000x

Chenyou Zhang,[a] Simran D. Kerai,[a] Tom Hawtrey,[b,c,d] Elizabeth J. New,[b,c,d] Markus Müllner[a,d,]*

Core–shell molecular polymer bottlebrushes (MPBs) were designed with a thermoresponsive poly(DEGMA) core and stabilising poly(PEGMA) shell. Solvatochromic fluorophores embedded in the core report polarity changes as it dehydrates and collapses upon heating, yielding a distinct fluorescence response. These stable, unimolecular nanostructures function as aqueous nanoscale sensors.

The properties of materials are often temperature dependent, and thus the development of approaches to probe temperature changes at different length scales has become a growing area of interest.[1–7] Nanothermometry – the measurement of temperature at the nanoscale – is dominated by inorganic and carbon-based nanomaterials, such as quantum and carbon dots, nanodiamonds and lanthanide nanoparticles.[8–13] Such particles tend to be intrinsically temperature-sensitive and therefore capable of reporting on temperature changes. Similarly, in the soft matters field, polymer nanoparticles utilising thermoresponsive polymers offer alternative approaches to temperatures sensing.[14–17] Many examples are focussed on linear (co)polymers comprising lower critical solution temperature (LCST) properties.[18–20] These polymers collapse at a certain temperature as polymer-solvent interactions weaken and polymer-polymer interactions become dominant. Decorating such polymers with environmentally-sensitive moieties (e.g. molecules responsive to changes in hydration) provides means to measure temperature changes. This is typically achieved with fluorophores that respond to changes in polymer solubility. Nevertheless, the precipitation of the polymer itself may result in a consequential barrier that limits the application of such systems, especially in nanomedicine and nanotechnology, where structural integrity and colloidal stability are important.[14,15] Stabilising the polymers with polyelectrolytes[16,21] or oligo(ethylene glycol)[22–24] has been shown to minimise this precipitation issue. However, these modifications will also alter the solution behaviour of polymers, resulting in multimolecular assemblies above the LCST due to the introduced amphiphilicity.[25]

To address these challenges, unimolecular polymer architectures, such as stars and bottlebrush polymers, are promising alternatives to linear polymers. As covalent unimolecular constructs, these nanomaterials can be designed to incorporate functional and stabilising compartments concurrently, ensuring stability whilst enabling functionality.[26–30] The opportunity to compartmentalise functionality in molecular polymer bottlebrushes (MPBs) has led to widespread adoption of MPBs as a versatile material class in polymer science, particularly for applications in self-assembly,[31–35] nanomedicine[36–38] and additive manufacturing.[39–41] The potential of MPBs to be used as thermometers at the nanoscale, however, has not yet been explored, notwithstanding their architectures providing an intrinsic ability to facilitate signal transduction without compromising the overall colloidal stability.

In this communication, we present the design and synthesis of compartmentalised MPBs, consisting of a functional core and stabilising shell **(Figure 1**). The poly(di(ethylene glycol) methyl ether methacrylate) core provides temperature-sensitive signal transduction through means of a solvatochromic fluorophore, whilst the poly(poly(ethylene glycol) methyl ether methacrylate) shell ensures colloidal stability. As a proof-of-concept, we demonstrate good correlation between temperature-induced expulsion of water from the core and solvatochromism, which demonstrates future potential for applications in thermometry.

Successful fluorophore attachment was confirmed through observation of strong fluorescence emission from **P3hf**, with two emission peaks corresponding to those exhibited by free **hfmal** (Supporting information, **Figure S1A**). The strong yellow colouration of the **P3hf** solution, which persisted even after extensive dialysis, further supported the successful fluorophore incorporation (**Figure S1B**). To verify the completion of deprotection and conjugation steps in the MPB, a linear

[a] *Key Centre for Polymers and Colloids, School of Chemistry, The University of Sydney, Sydney, NSW 2006, Australia.*
[b] *School of Chemistry, The University of Sydney, Sydney, NSW 2006, Australia.*
[c] *Australian Research Council Centre of Excellence for Innovations in Peptide and Protein Science, The University of Sydney, Sydney 2006 NSW Australia*
[d] *The University of Sydney Nano Institute (Sydney Nano), Sydney, NSW 2006, Australia.*

Supplementary Information available: [details of any supplementary information available should be included here]. See DOI: 10.1039/x0xx00000x

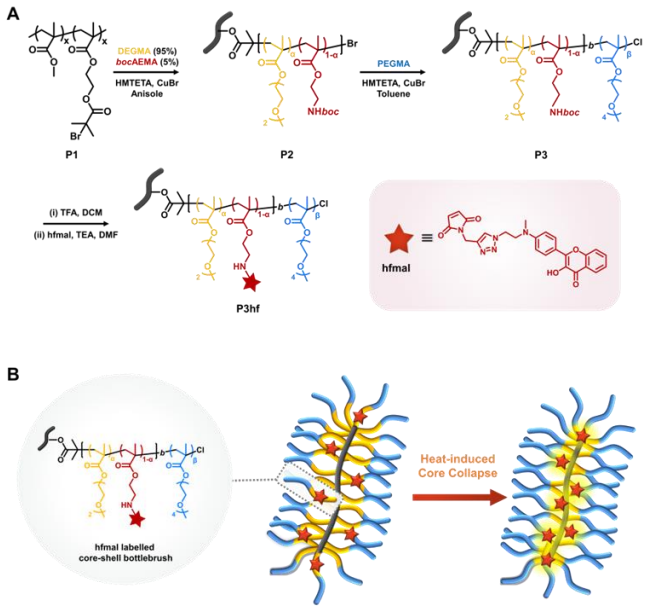

Figure 1. Route to a unimolecular thermal responsive core shell polymer bottlebrush. (A) Synthetic route to the core-shell bottlebrush thermometer. (B) Representative mechanism of signal transduction on thermal stimulus.

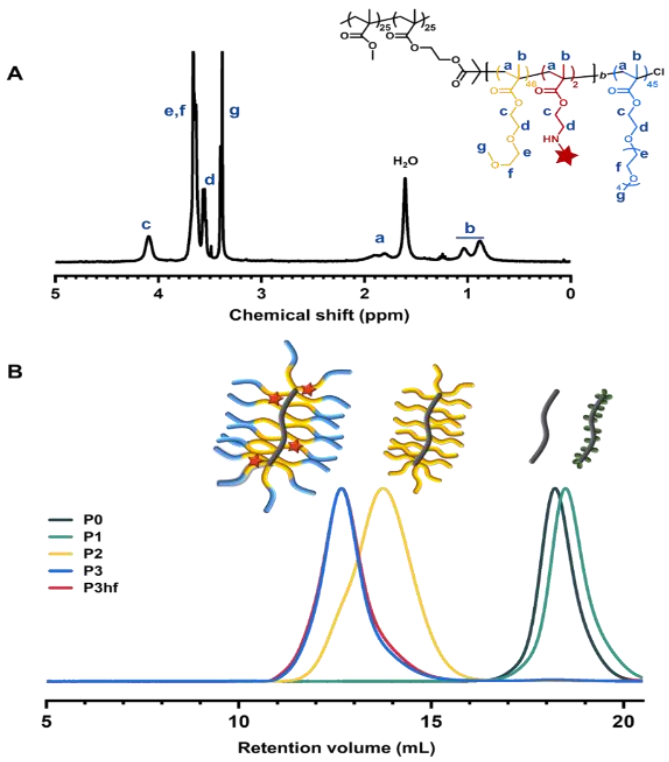

Figure 2. (A) ^{1}H NMR spectrum and structure of **P3hf**. (B) SEC elugrams (50 °C, 1 mL/min, DMAc) of **P1**(green), **P0** (navy), **P2** (yellow), **P3** (blue), and **P3hf** (red).

copolymer analogue, poly(DEGMA$_{42}$-*co*-*boc*AEMA$_2$) was synthesised, allowing clear observation of the *boc* deprotection and subsequent fluorophore attachment via ^{1}H NMR spectroscopy (**Figure S2**). All polymers were synthesised under well-controlled polymerisation conditions and displayed monomodal molecular weight distributions, summarised in **Table 1**.

Figure 2A shows a representative ^{1}H NMR spectrum of **P3hf**. SEC confirmed a steady growth of hydrodynamic volume with each synthesis step (**Figure 2B)**. The representative ^{1}H NMR spectra of **P0**, **P1**, **P2** and **P3** can be found in the Supporting Information. Hydrodynamic size distributions of MPBs were characterised using dynamic light scattering (DLS) and atomic force microscopy (AFM) with good agreement (**Figure 3**).

Since **hfmal** is an excited state intramolecular proton transfer (ESIPT) solvatochromophore with distinct fluorescent emissions arising from its tautomeric forms, alteration of solvent polarity ratiometrically changes its emission behaviour[42] (**Figure S1A**, in a gradually altered solvent system, and **Figure S3** in different solvents),[43,44] we next sought to assess the fluorescence behaviour of our MPBs in response to temperature changes.

Table 1. Overview of synthesis and characterisation data of MPBs obtained *via* ATRP.

Polymer	Composition	Conversion (%) [a]	Feed ratio [b]	$M_{n,NMR}$ (kg/mol) [a]	$M_{n,SEC}$ (kg/mol) [c]	$Đ$ [c]	Hydrodynamic diameter (nm) [d]
P0	PMMA$_{25}$-*co*-PHEMA$_{25}$	99	[1]:[25/25]:[1.5]:[1.1] (Cl)	5.95	12.5	1.15	-
P1	PMMA$_{25}$-*co*-PBIEM$_{25}$	-	-	9.68	11.9	1.21	-
P2	**P1**-*g*-PDEGMA$_{46}$-*co*-P*boc*AEMA$_2$	24	[1]:[190/10]:[2]:[1.2] (Br)	238	150	1.20	22
P3	**P2**-*b*-PPEGMA$_{45}$	23	[1]:[200]:[4]:[2] (Cl)	575	282	1.17	33

[a] Conversion was determined by ^{1}H NMR, $M_{n,NMR}$ calculated considering 100% grafting efficiency from **P1**. [b] [Polyinitiator]:[monomer]:[ligand]:[copper halide] (halide) feed molar ratio of the polymerisations via ATRP. [c] Apparent average molecular weight M_n obtained from DMAc SEC using monodisperse PMMA calibration standards. [d] Z-average of DLS measurements of polymers in deionised water at 5 ºC.

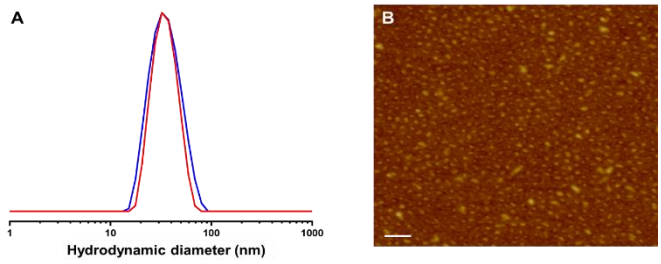

Figure 3. (A) Intensity-weighted DLS results of **P3** (1 g/L, deionised water) at 7 °C (blue) and 36 °C (red). Apparent hydrodynamic diameter is centred around 32 nm. (B) AFM height image of **P3hf** prepared from methanol. z-Scale = ±5 nm. Scale bar = 100 nm.

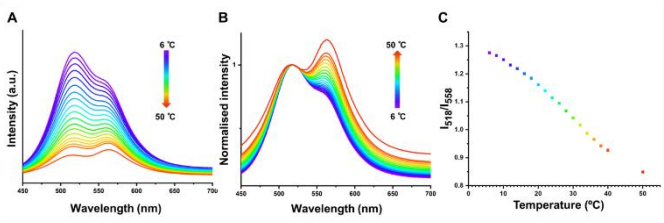

Figure 4. Fluorescence emission spectra of P3hf (1 g/L, deionised water, λ_{ex} = 400 nm) at different temperatures from 6 °C (blue) to 40 °C (orange) at 2 °C increments. A 50 °C measurement was also obtained to probe the range of response. (A) unmodified emission spectra of aqueous P3hf solution, (B) normalised spectra, normalised to the 518 nm emission, (C) plot of ratios of emission peaks (I_{518}/I_{558}) against temperature.

The PDEGMA core (**P2**) is thermoresponsive and will collapse with increasing temperature beyond the LCST, as verified with prior DLS experiments (**Figure S4 and S5**). This collapse is expected to lead to an expulsion of water from the core, cascading to changing compartment polarity, actuating solvatochromism, which alters the fluorescence response of the conjugated probe. Thus, a solution of **P3hf** was heated from 6 °C to 40 °C in 2 °C increments, where the PDEGMA core underwent the expected dehydration, changed the local environment of the fluorophore, and demonstrated a ratiometric response to the temperature increase (**Figure 4**).

Upon heating, the emission intensity of **P3hf** decreased steadily with rising temperature (**Figure 4A**), accompanied by a decrease in the ratio of the emission peaks (I_{518}/I_{558}, **Figure 4C**). This behaviour was not observed for free **hfmal** (**Figure S6**), indicating that the temperature-induced fluorescence changes from **P3hf** system can be attributed to the attenuation of polarity within its thermoresponsive core to which the fluorophore was attached. Pearson's r from regression analysis between the emission ratio and temperature revealed a strong inverse linear relationship (r = -0.9959, **Figure S7A**). In single-blind verifications of **P3hf**, the obtained ratio and calculated temperature were in good agreement with the abovementioned relationship, indicating promising potential thermometry applications (**Figure S7**). As the temperature increases, the relative decrease in polarity altered the ratiometric emission behaviour of the dye. This then transformed the usability of the dye as changes in the emission ratio are now a reliable indicator of the surrounding temperature.

To gain a mechanistic understanding of the thermal response of the core in **P3hf**, we compared it to that of the constituent **P2** by dynamic light scattering (DLS, 1 g/L, deionised water). **P2** exhibited a phase transition temperature (Tpt) – as indicated by a sudden increase in apparent size – between 13-15 °C (**Figure S4**). The Tpt is lower than previously reported values for linear PDEGMA,[6,24,45] likely due to the bottlebrush architecture,[23] and copolymerisation of hydrophobic *boc*AEMA.[46,47] DLS studies of **P3** (1 g/L, deionised water) revealed a different picture, with no significant change in apparent hydrodynamic size up to 40 °C (**Figure S8**). This temperature ceiling was selected to be below the LCST of the PEGMA shell at approximately 55 °C,[23,46] as well as being physiologically relevant. The absence of aggregation and significant volume changes with changing temperature indicates that the PEGMA shell provides sufficient shielding from the collapsing core and retains the unimolecular character at elevated temperatures. This is supported by previous experimental and computational studies on copolymers of linear PDEGMA-*co*-POEGMA in both random and block copolymers.[6,8,48] Of particular interest is the block copolymer behaviour, while the PDEGMA block undergoes coil to globular transition, aggregation is suppressed by the PPEGMA block via steric interactions.[8,48] Hence, the ratiometric change as reported by **P3hf** (**Figure 4A**) can be attributed to the dehydration of the PDEGMA core block leading to alteration of local environment polarity. Previously reported simulation studies have also indicated further dehydration of polymers above LCST, indicated by reduction in number of associated hydrogen bonds,[48,49] aligning with the transient response in ratiometric terms past the LCST observed for PDEGMA within **P3hf**.

In summary, this work introduced a unimolecular core-shell MPB capable of sensing temperature changes within its core. The bottlebrush nanomaterial was designed to exhibit a strong linear correlation between ratiometric fluorescent response and temperature changes. The presented proof-of-concept study provides a basis for further improvement of sensitivity, for example through different fluorophores and core functionality. Moreover, we anticipate utility as unimolecular thermometers for cell studies or as additives in polymer networks.

Our research was facilitated by access to Sydney Analytical, a core research facility at the University of Sydney. The authors acknowledge the technical and scientific assistance from Sydney Microscopy & Microanalysis, the University of Sydney node of Microscopy Australia. C.Z. is grateful to Dr Haoxiang Zeng and Dr Yen Theng Cheng for valuable discussions. We thank Professor Ronald Clarke for access to the fluorometer, and Professor Chiara Neto for access to an atomic force microscope. C.Z. gratefully acknowledges the L E R Tonnet and Family Scholarship in Chemistry, and a supplementary scholarship from the School of Chemistry, University of Sydney. S.D.K. is a recipient of an Australian Government RTP scholarship. M.M. acknowledges the Australian Research Council for a Future Fellowship (FT200100185), Discovery Project (DP220100452), and LIEF grant (LE240100091), respectively. M.M. is a grateful recipient of a Global Science and Technology Diplomacy Fund (GSTDS000001 – 6) grant.

Conflicts of interest

There are no conflicts to declare. MM conceived the idea. CZ and MM conceptualised the project. CZ designed, synthesised, characterised, and analysed polymers, its modifications, and responses. SDK performed AFM and single blind experiments. TH synthesised and characterised the fluorophore under supervision from EJN. CZ and MM co-wrote the manuscript, with input from all authors.

Data availability

The data supporting this article have been included as part of the Supplementary Information.

Notes and references

1 G. Kucsko, P. C. Maurer, N. Y. Yao, M. Kubo, H. J. Noh, P. K. Lo, H. Park and M. D. Lukin, *Nature*, 2013, **500**, 54–58.
2 K. M. McCabe and M. Hernandez, *Pediatr. Res.*, 2010, **67**, 469–475.
3 J. Lee and N. A. Kotov, *Nano Today*, 2007, **2**, 48–51.
4 L. Đačanin Far and M. Dramićanin, *Nanomaterials*, 2023, **13**, 2904.
5 S. Uchiyama and C. Gota, *Rev. Anal. Chem.*, 2017, **36**, 20160021.
6 J. Bassi da Silva, P. Haddow, M. L. Bruschi and M. T. Cook, *J. Mol. Liq.*, 2022, **346**, 117906.
7 H. Zhu, H. Xu, Y. Zhang, J. Brodský, I. Gablech, M. Korabečná and P. Neuzil, *Adv. Sci.*, 2025, **12**, 2402135.
8 F. Ye, C. Wu, Y. Jin, Y.-H. Chan, X. Zhang and D. T. Chiu, *J. Am. Chem. Soc.*, 2011, **133**, 8146–8149.
9 M. Jia, X. Chen, R. Sun, D. Wu, X. Li, Z. Shi, G. Chen and C. Shan, *Nano Res.*, 2023, **16**, 2949–2967.
10 H. Liu, Y. Fan, J. Wang, Z. Song, H. Shi, R. Han, Y. Sha and Y. Jiang, *Sci. Rep.*, 2015, **5**, 1–8.
11 A. G. Bispo-Jr, L. F. Saraiva, S. A. M. Lima, A. M. Pires, I. O. Mazali and F. A. Sigoli, *J. Mater. Chem. C*, 2025, **13**, 3320–3330.
12 Y. S. Kato, Y. Shimazaki, S. Chuma, K. Shiraya, Y. Nakane, T. Sugi, K. Okabe, Y. Harada and S. Sotoma, *Nano Lett.*, 2025, **25**, 5688–5696.
13 Y. Lee, K. Kim, D. Kim and J. S. Lee, *J. Am. Chem. Soc.*, 2025, **147**, 13180–13189.
14 S. Uchiyama, Y. Matsumura, A. P. de Silva and K. Iwai, *Anal. Chem.*, 2003, **75**, 5926–5935.
15 C. Pietsch, A. Vollrath, R. Hoogenboom and U. S. Schubert, *Sensors*, 2010, **10**, 7979–7990.
16 K. Okabe, N. Inada, C. Gota, Y. Harada, T. Funatsu and S. Uchiyama, *Nat. Commun.*, 2012, **3**, 705.
17 C. Gota, K. Okabe, T. Funatsu, Y. Harada and S. Uchiyama, *J. Am. Chem. Soc.*, 2009, **131**, 2766–2767.
18 C. Pietsch, U. S. Schubert and R. Hoogenboom, *Chem. Commun.*, 2011, **47**, 8750–8765.
19 Y. Yuan, K. Raheja, N. B. Milbrandt, S. Beilharz, S. Tene, S. Oshabaheebwa, U. A. Gurkan, A. Cristina, S. Samia and M. Karayilan, *RSC Appl. Polym.*, 2023, **1**, 158–189.
20 G. Nunziata, M. Nava, E. Lacroce, F. Pizzetti and F. Rossi, *Macromol. Rapid Commun.*, 2025, **46**, 2401127.
21 Z. Chen, K. Y. Zhang, X. Tong, Y. Liu, C. Hu, S. Liu, Q. Yu, Q. Zhao and W. Huang, *Adv. Funct. Mater.*, 2016, **26**, 4386–4396.
22 X. Hu, Y. Li, T. Liu, G. Zhang and S. Liu, *ACS Appl. Mater. Interfaces*, 2015, **7**, 15551–15560.
23 P. Ramamurthi, Z. Zhao, E. Burke, N. F. Steinmetz, M. Müllner, *Adv. Healthc. Mater.*, 2022, **11**, 2200163.
24 C. Porsch, S. Hansson, N. Nordgren and E. Malmström, *Polym. Chem.*, 2011, **2**, 1114–1123.
25 F. Ercole, S. Harrisson, T. P. Davis and R. A. Evans, *Soft Matter*, 2011, **7**, 2687–2696.
26 M. F. Fouz, K. Mukumoto, S. Averick, O. Molinar, B. M. McCartney, K. Matyjaszewski, B. A. Armitage and S. R. Das, *ACS Cent. Sci.*, 2015, **1**, 431–438.
27 E. W. Kent, D. M. Henn and B. Zhao, *Polym. Chem.*, 2018, **9**, 5133–5144.
28 B. Zhao, *J. Phys. Chem. B*, 2021, **125**, 6373–6389.
29 T. Pelras, C. S. Mahon and M. Müllner, *Angew. Chemie - Int. Ed.*, 2018, **57**, 6982–6994.
30 M. Müllner and A. H. E. Müller, *Polymer*, 2016, **98**, 389–401.
31 H. Zeng, P. Zeng, J. Baek, B. S. Kim and M. Müllner, *Angew. Chemie Int. Ed.*, 2025, **64**, e202424269.
32 H. Zeng, X. Liang, D. A. Roberts, E. R. Gillies and M. Müllner, *Angew. Chemie Int. Ed.*, 2024, **63**, e202318881.
33 Z. Li, M. Tang, S. Liang, M. Zhang, G. M. Biesold, Y. He, S. M. Hao, W. Choi, Y. Liu, J. Peng and Z. Lin, *Prog. Polym. Sci.*, 2021, **116**, 101387.
34 F. Shao, Y. Wang, C. M. Tonge, E. R. Sauvé and Z. M. Hudson, *Polym. Chem.*, 2020, **11**, 1062–1071.
35 C. Vu, N. Abu Amara, M. Alaboalirat, E. Nativ-Roth, R. Zalk, W. Leite, J. Carrillo, R. Bitton and J. B. Matson, *Angew. Chemie*, 2025, **64**, e202500771.
36 M. Müllner, *Macromol. Chem. Phys.*, 2016, **217**, 2209–2222.
37 M. Müllner, *Chem. Commun.*, 2022, **58**, 5683–5716.
38 A. Niederberger, T. Pelras, L. S. Manni, P. A. FitzGerald, G. G. Warr and M. Müllner, *Macromol. Rapid Commun.*, 2021, **42**, 1–6.
39 J. Rzayev, *ACS Macro Lett.*, 2012, **1**, 1146–1149.
40 Z. Jin, H. G. Seong, S. Srivastava, A. McGlasson, T. Emrick, M. Muthukumar and T. P. Russell, *Angew. Chemie - Int. Ed.*, 2024, **63**, e202404382.
41 S. Jeon, Y. L. Kamble, H. Kang, J. Shi, M. A. Wade, B. B. Patel, T. Pan, S. A. Rogers, C. E. Sing, D. Guironnet and Y. Diao, *Proc. Natl. Acad. Sci.*, 2024, **121**, 2017.
42 C. Y. Chen and C. T. Chen, *Chem. Commun.*, 2011, **47**, 994–996.
43 A. S. Klymchenko, V. G. Pivovarenko and A. P. Demchenko, *J. Phys. Chem. A*, 2003, **107**, 4211–4216.
44 P.-T. Chou, M. L. Martinez and J. H. Clements, *J. Phys. Chem*, 1993, **97**, 2618–2622.
45 S. I. Yamamoto, J. Pietrasik and K. Matyjaszewski, *Macromolecules*, 2007, **40**, 9348–9353.
46 A. P. Constantinou, B. Zhan and T. K. Georgiou, *Macromolecules*, 2021, **54**, 1943–1960.
47 Q. Li, L. Wang, F. Chen, A. P. Constantinou and T. K. Georgiou, *Polym. Chem.*, 2022, **13**, 2506–2518.
48 E. Dalgakiran and H. Tatlipinar, *J. Phys. Chem. B*, 2019, **123**, 1283–1293.
49 Z. Ye, H. Su, C. Lian, J. Hu, Y. Shang and H. Liu, *Mol. Simul.*, 2021, **47**, 299–305.

